applied sciences

MDPI

Article

Laser Fabrication of Titanium Alloy-Based Photothermal Responsive Slippery Surface

Jian Yi, Hao Zhou, Xingchen Han, Jiangwei Mao and Yonglai Zhang *

State Key Laboratory of Integrated Optoelectronics, College of Electronic Science and Engineering, Jilin University, 2699 Qianjin Street, Changchun 130012, China; yijian2102132@163.com (J.Y.); zhouhao21@mails.jlu.edu.cn (H.Z.); hanxc21@mails.jlu.edu.cn (X.H.); maojw20@jlu.edu.cn (J.M.)
* Correspondence: yonglaizhang@jlu.edu.cn

Abstract: In recent years, biomimetic materials inspired from natural organisms have attracted great attention due to their promising functionalities and cutting-edge applications, emerging as an important research topic. For example, how to reduce the reflectivity of the solid surface and increase the absorption of the substrate surface is essential for developing light response smart surface. Suitable solutions to this issue can be found in natural creatures; however, it is technologically challenging. In this work, inspired from butterfly wings, we proposed a laser processing technology to prepare micro nanostructured titanium alloy surfaces with anti-reflection properties. The reflectivity is significantly suppressed, and thus, the light absorption is improved. Consequently, the anti-reflection titanium alloy surface can be further employed as a photothermal substrate for developing light-responsive slippery surface. The sliding behavior of liquid droplets on the smart slippery surface can be well controlled via light irradiation. This method facilitates the preparation of low-reflection and high-absorption metallic surfaces towards bionic applications.

Keywords: bionics; laser micro-/nanofabrication; anti-reflection structure; slippery surface

check for updates

Citation: Yi, J.; Zhou, H.; Han, X.; Mao, J.; Zhang, Y. Laser Fabrication of Titanium Alloy-Based Photothermal Responsive Slippery Surface. *Appl. Sci.* **2022**, *12*, 608. https://doi.org/10.3390/app12020608

Academic Editors: Jianlei Cui, Wenjun Wang and Xuesong Mei

Received: 20 November 2021
Accepted: 24 December 2021
Published: 9 January 2022

Publisher's Note: MDPI stays neutral with regard to jurisdictional claims in published maps and institutional affiliations.

Copyright: © 2022 by the authors. Licensee MDPI, Basel, Switzerland. This article is an open access article distributed under the terms and conditions of the Creative Commons Attribution (CC BY) license (https://creativecommons.org/licenses/by/4.0/).

1. Introduction

Functional materials inspired from the surface structures of organisms show new research trends [1–3]. There are already many bionic prototypes, such as "lotus leaf", "butterfly wings", "nepenthes", etc. Imitating these natural structures can effectively promote the development of artificial functional materials and surfaces [4–8]. For instance, the surface micro-nanostructures of the wing butterfly has the characteristics of electrical response and can be used in the field of electro-induced stealth [9]; the wing-scale photonic crystal structures of the Paradise Swallowtail butterfly can produce a reversible thermochromic reaction with the change of the external refractive index [10]. The slippery surface of Nepenthes has good hydrophobic properties, better stability, and the advantages of waterproof, antifouling, high-temperature, and high-pressure stability, etc. [11,12], which can be applied to industrial fields, such as biomedical equipment, blood catheters, and marine antifouling. In recent years, the Nepenthes-inspired functional surfaces with stimuli-responsive properties have been proven interesting and versatile smart surfaces in both fundamental science and practical applications [13–15]. Therefore, it is highly desired to develop biomimetic slippery surface structures with lubricating characteristics based on stimuli-responsive materials.

Laser processing enables high-precision and designable fabrication of hierarchical micro-nanostructures on various functional materials, revealing great potential for developing biomimetic surface and devices [16–20]. With the help of laser processing, biomimetic structures can be readily produced on different materials according to the models of natural creatures [21–24]. The surface microstructures and nanostructures of metal surface are essential for their potential applications in different fields, for instance, anti-icing, corrosion

resistance, heat radiation, and anti-reflection [25–29]. Especially considering the camouflage and photothermal applications, great efforts have been devoted to the development of laser-induced metallic anti-reflection surfaces [30]. For example, Fan et al. proposed and proved through experiments that a highly disordered, super hierarchical micro-nano structure formed on the surface of a metal (such as Cu) exhibits a high degree of anti-reflection ability in the ultra-broadband spectrum from ultraviolet to far infrared [31]. Zheng et al. proposed a hybrid method consisting of ultra-fast laser-assisted texturing and chemical fluorination treatment to significantly reduce the reflectivity of the titanium alloy surface by creating ultra-light trapping micro-nano structures [32]. In spite of these pioneering works, innovations on rational design and fabrication of anti-reflective micro-nano structures through a biomimetic manner are still highly desired. Open problems with respect to the reduction of reflectivity, the increase of light absorption, and especially the applications of anti-reflection metal surface in different fields are still challenging.

In this work, we propose the laser fabrication of anti-reflection titanium alloy surface and its applications in developing light-responsive slippery surface. Laser processing has been employed to create anti-reflection structures, similar to the black region of Little Angel Swallowtail Butterfly wings, on titanium alloy through a laser ablation and nanoparticle deposition process. The laser-structured titanium alloy surface demonstrates good anti-reflection properties (300~2000-nm reflection smaller than 10%) and improved light absorption ability. In addition, the anti-reflection titanium alloy surface is employed as a photothermal substrate to prepare a light-responsive slippery surface, which can be used to control the sliding behavior of liquid droplets. This method enables the preparation of anti-reflection and high-absorption metal surfaces, revealing great potential for applications in bionic devices and microfluidics.

2. Methods

2.1. Sample Preparation

A 40 mm × 40 mm × 1 mm titanium alloy slice was used for sample preparation. First, it was cleaned with ethanol before laser processing. The laser treatment mode was set to the laser ablation mode to fabricate micro-nano-structures on the titanium alloy surface. The parameters were set as: scanning speed 50 mm/s, frequency 20 kHz, power 10 W. The scheme for laser processing process is shown in Figure 1a. Figure 1b shows a schematic diagram of the reflection of light on smooth surface and the anti-reflection effect on the laser-structured surface. Briefly, the antireflection effect can be attributed to the grooved microstructures and the nanoscale roughness on the surface.

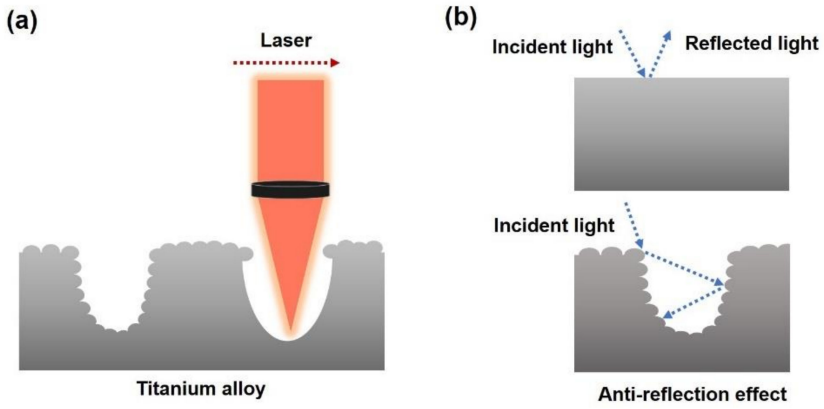


Figure 1. Schematic diagram of (**a**) laser treatment of titanium alloy surface and (**b**) surface anti-reflection effect.

2.2. Characterization

The scanning electron microscope (SEM)image was obtained by JEOL field emission scanning electron microscope (JSM-7500). The temperature data were obtained from a

non-contact infrared thermometer (smart sensor AS872D). The relative thermal image was taken with an infrared camera called FLIR One. The titanium alloy samples prepared under different laser-processing conditions were placed under the lamp, and the non-contact infrared thermometer monitored the rise of surface temperature under light irradiation in real time. Confocal laser scanning microscope (CLSM)images were obtained from LEXT 3D measurement laser microscope (OLS4100).

3. Results and Discussion

3.1. Butterfly Wings Model

Figure 2a shows a specimen of a Little Angel Swallowtail Butterfly. We observed the black region on the butterfly wing and investigated the surface structures on the scales using the confocal microscope. The microscopic image is shown in Figure 2b; it can be seen from the image that scales are neatly arranged on the butterfly wings. Each scale is curved and overlapped, with distinct linear grooves in the scales. This unique anisotropic microstructure accounts for their surface wettability. Interestingly, the actual color of the dark region observed with the naked eye is brown-yellow. Nevertheless, since the linear grooves on the butterfly wings effectively absorb incident light and have an obvious anti-reflection effect, the brown-yellow area of the butterfly wing appears black to the naked eyes. In addition, the butterfly's layered wings may also play a role in the anti-reflection effect. To get deep insight into the anti-reflection effect of a butterfly wing, we further investigated the photothermal effect of the wing under light irradiation, as shown in Figure 2c,d.

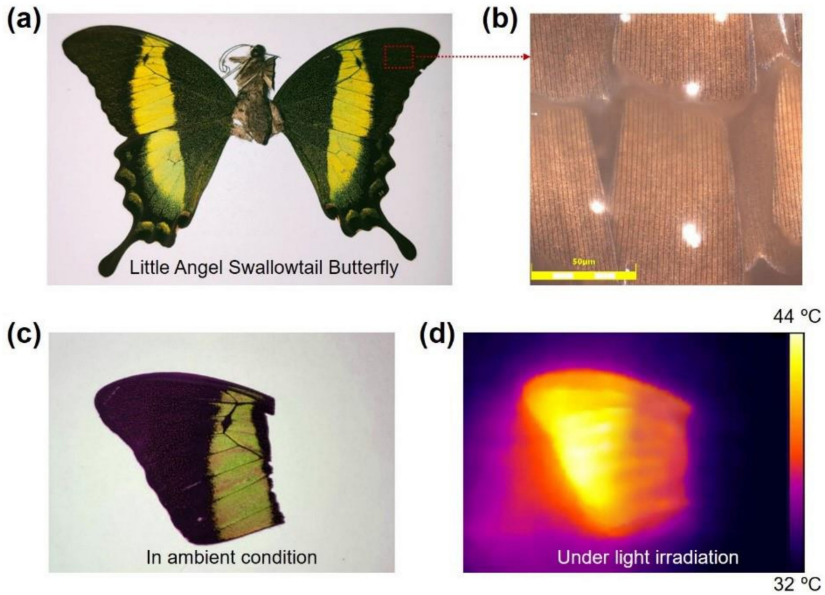


Figure 2. (**a**) Photograph of a butterfly. (**b**) CLSM images of the butterfly wings. (**c**) Photography of a fragment of butterfly wings. (**d**) Photothermal image of the fragment under light irradiation.

3.2. Surface Microscopy

Figure 3 shows the surface morphology of the laser structured titanium alloy. As shown in Figure 3a, after laser treatment, the laser-treated region becomes black, while the untreated region shows obvious metallic luster. The darkness of the laser-treated region suggests the anti-reflection effect. To get deep insight into the microstructures of the laser-treated and untreated region, we further characterized the sample with CLSM. Figure 3b shows the CLSM image of the untreated region of the titanium alloy substrate. It can be seen from the image that the surface is not very smooth, with a small number of irregular depressions on the surface. In spite of the surface roughness, the sample appears smooth as a whole. Figure 3c shows the CLSM image and the surface profile (Figure 3d,e) of the laser-processed region. The as-formed microstructures are inspired from the scales of a

butterfly wing. There are protrusions and linear grooves, which are comparable to the grooves of butterfly wings. In addition, the grooved microstructures are also not smooth; there are plenty of nanoparticles on the surface. This rough and grooved microstructures and can effectively absorb light and thus reduce reflection.

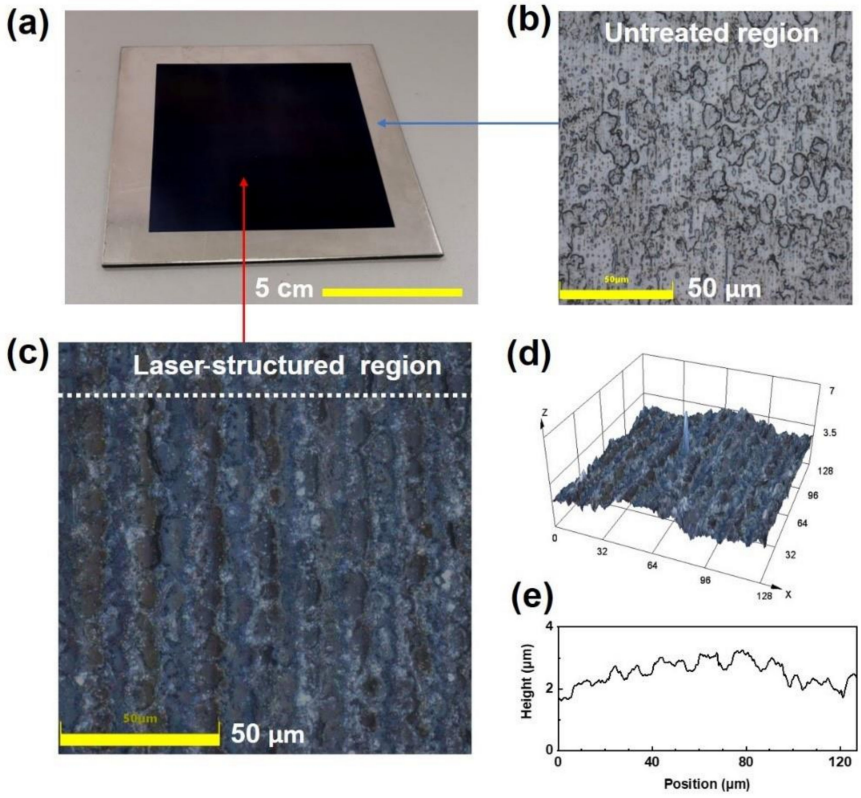


Figure 3. (**a**) Photograph of a laser-treated titanium alloy surface. (**b**) CLSM image of the untreated region of the titanium alloy substrate. (**c**) CLSM image, (**d**) 3D topography and (**e**) cross-section height curve of the laser-treated region of the titanium alloy substrate.

Figure 4a–c are the SEM images of the initial titanium alloy sample. It can be clearly seen from the figure that the surface of the untreated sample presents a smooth morphology. Figure 4d–f are SEM scanning photos of the sample after laser processing. It can be seen that the sample after laser processing has obvious protrusions and grooves, accompanied by granular material attached to the sample surface. Further magnification of a granular attachment reveals a stack of irregular bulges. When these irregular bumps are further magnified, the nanoporous structure can be clearly observed. The hierarchical micro-nanostructures are very helpful for light trapping. When light illuminates the sample, the hierarchical micro-nanostructures can effectively capture the incident light and perform multiple reflections inside, effectively reducing the light reflection to the surface. Therefore, the laser-treated sample is black in color, demonstrating obvious anti-reflection effect.

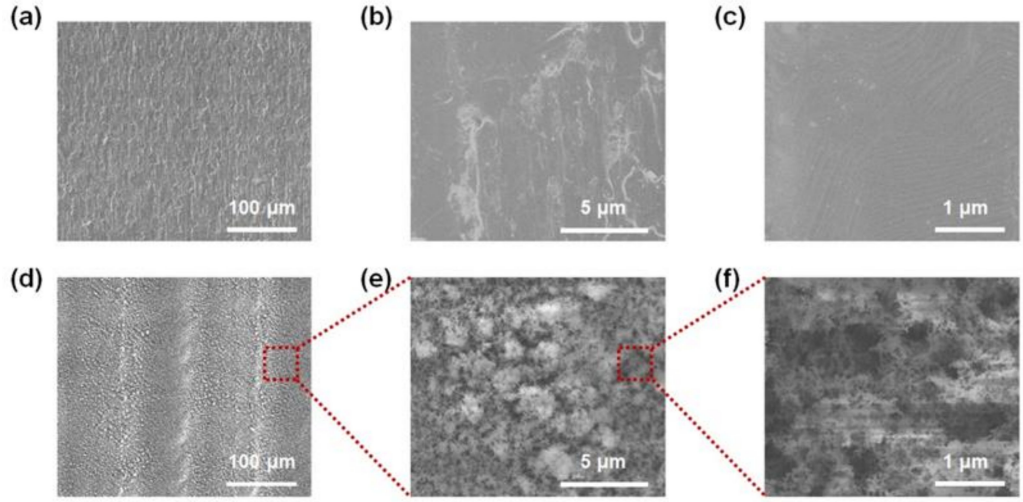


Figure 4. (**a**–**c**) SEM images of initial titanium alloy substrate. (**d**–**f**) SEM images of laser-treated titanium alloy substrate.

3.3. Reflection

To make a direct comparison of the reflection effect between laser-treated and untreated region, we collected the reflectance spectra. Figure 5 shows the surface reflectance spectra of the untreated sample and the sample after laser processing. It can be seen from the figure that the reflectivity of the untreated sample is ~50% between 800 and 200 nm. This means about half of the light can be reflected. The reflection of IR light may result in loss half of the light energy irradiated on the surface. In this case, the photothermal conversion rate is not high. On the contrary, the reflectivity of the laser-treated sample from 300 to 2000 nm is less than 8%. The lowest reflectivity around 500 nm is only 2%. At the same time, it can be seen from the figure that the reflection intensity of the laser-processed sample is much lower than that of the initial sample. It can be preliminarily judged that the sample after laser processing shows much higher anti-reflection effect, which promotes light absorption and the light-heat conversion. Therefore, under stable light source conditions, more light energy can be harvested from the laser-treated titanium alloy surface.

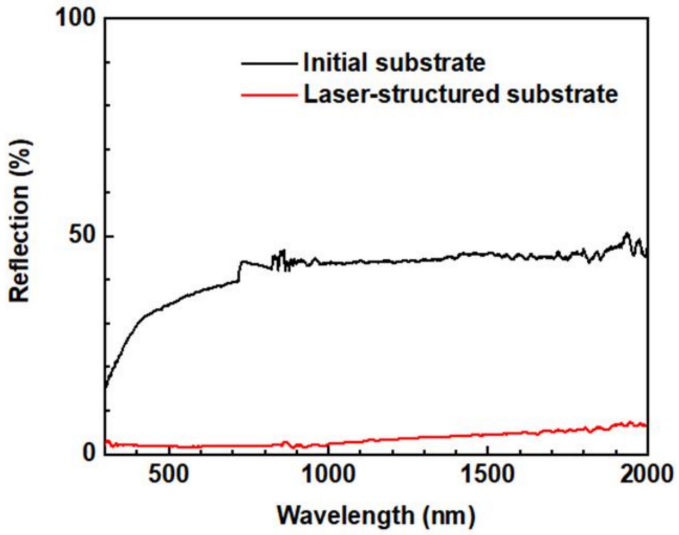


Figure 5. Surface reflectance spectra of initial titanium alloy substrate and laser-treated titanium alloy substrate.

3.4. Photothermal Property

To investigate the photothermal conversion effect, we placed the initial titanium alloy sample and the laser-processed one under a stable light source for 10 min and recorded

the surface temperature with a thermal imaging lens. To make a clear comparison, we fabricated a pattern on titanium alloy surface. The results are shown in Figure 6a. It is obvious from the figure that the temperature of the laser-treated region is much higher than that of the untreated region. Consequently, it can be concluded that the photothermal conversion efficiency of the laser-treated sample is much higher than that of the untreated sample. The improved photothermal effect with respect to the laser-treated sample can be attributed to the anti-reflection property. Figure 6b shows the temperature-rising curve of the sample. Under the same initial temperature, the untreated sample and the laser-treated sample are irradiated under the same light source for 540 s. The results show that the temperature of the sample increased with the irradiation time. Notably, the temperature of the untreated sample increased from 15.5 °C to 30.1 °C within 60 s. With the increase of irradiation time, the temperature rose slowly, and the final temperature tended to be stable around 40.5 °C. On the contrary, the temperature of the laser-treated sample increased from 15.5 °C to 40.5 °C within 60 s. The temperature rise was much higher than that of the untreated sample. After irradiation for 600 s, the temperature rose to ~65 °C. The anti-reflection property of the laser-treated sample promotes the light absorption, and thus, the surface temperature rises under light irradiation is faster and higher. Due to the anti-reflection effect, the light-utilization rate with respect to the laser-treated titanium alloy is also improved. We also tested the photothermal properties of the paraffin coated structured titanium alloy surface. After coating paraffin, the photothermal property nearly changes because of the thin paraffin film.

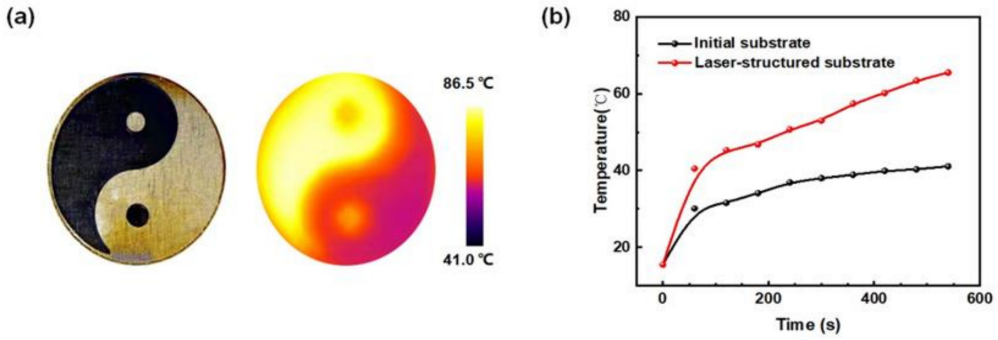


Figure 6. (**a**) Thermal imaging of initial titanium alloy and laser-treated titanium alloy substrate. (**b**) Dependence of the surface temperature on irradiation time for initial titanium alloy and laser-treated titanium alloy substrate.

3.5. Wettability

Figure 7a is the static contact angle histogram of the sample at room temperature. It can be seen that the initial contact angle of the sample is 58.4°. In the sample after laser processing, the contact angle measured from the direction perpendicular and parallel to the groove was 54.2° and 65.2°, respectively. These results show that the titanium alloy sample before and after laser treatment are both hydrophilic. To fabricate the photothermally responsive slippery surface, paraffin was placed on the laser-treatment surface. After heating, the paraffin was melted and coated the laser-treatment surface. As shown in the Figure 7b, the liquid can slide on the slippery surface upon light irradiation.

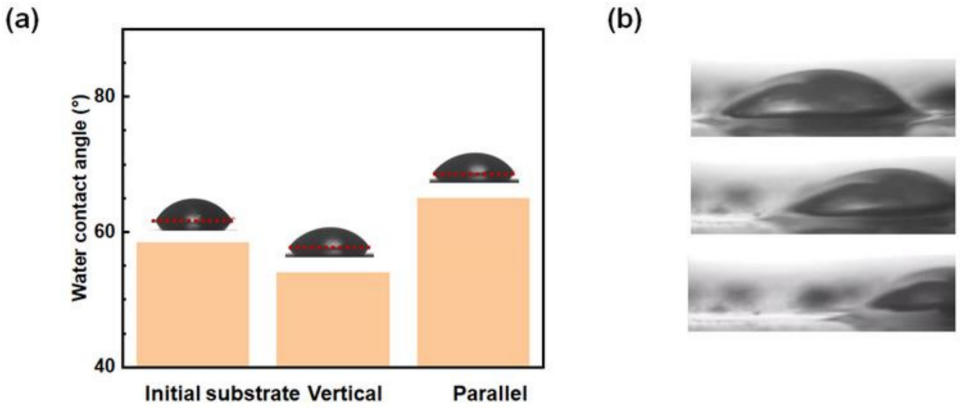


Figure 7. (**a**) The contact angle of the initial sample and the laser processed sample. (**b**) The surface droplet sliding.

Figure 8a is the schematic diagram of the droplet sliding on the sample surface under light irradiation [33]. There is a high adhesion between water droplets and paraffin. The water droplets can be pinned on the paraffin surface. When exposed to light, the laser-treated titanium alloy will undergo photothermal conversion to melt the paraffin on the surface. Therefore, when irradiated by light, the paraffin will melt. The material surface will become a slippery surface. The adhesion of water droplets to the substrate surface will be reduced, resulting in water droplet sliding (Figure 8b).

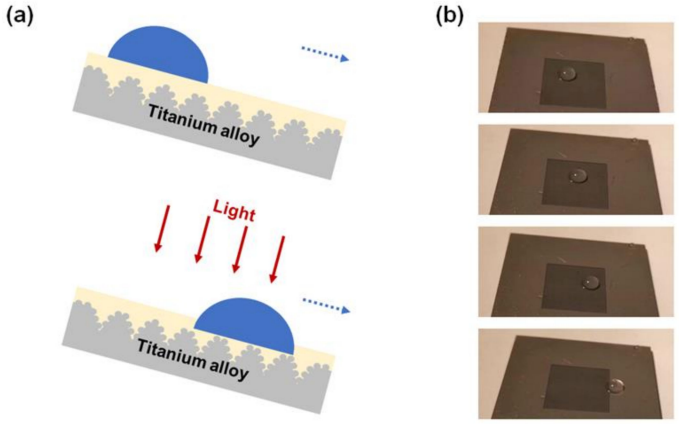


Figure 8. (**a**) Schematic diagram of the droplet sliding on the sample surface after laser processing under light irradiation. (**b**) Droplet sliding on the sample surface under light irradiation.

4. Conclusions

In this work, we prepared a hierarchically structured titanium alloy surface with good anti-reflection property via laser treatment. The reflectivity of the untreated sample is ~50% between 800 and 200 nm, whereas the reflectance of the structured sample is less than 10% from 300 to 2000 nm. CLSM and SEM images show that the surface of the sample has micro-scale grooves and nanoporous structures, and the hierarchical structures play a vital role in the anti-reflection effect. Furthermore, we also used a simple method to obtain a slippery surface with good hydrophobicity. This method will be beneficial to the preparation of high-absorption metal surface materials or used in the field of microfluidic chips.

Author Contributions: Conceptualization, Y.Z.; investigation, J.Y., H.Z., X.H. and J.M.; validation, Y.Z.; formal analysis, J.Y. and Y.Z.; writing—original draft preparation, J.Y.; writing—review and editing, J.Y. and Y.Z.; supervision, Y.Z.; project administration, Y.Z.; funding acquisition, Y.Z. All authors have read and agreed to the published version of the manuscript.

Funding: This research was funded by the National Natural Science Foundation of China (61935008, 61775078).

Data Availability Statement: The data used to support the findings of this study are available from the corresponding author upon request.

Conflicts of Interest: The authors declare no conflict of interest.

References

1. Zhang, Y.L.; Liu, Y.Q.; Han, D.D.; Ma, J.N.; Wang, D.; Li, X.B.; Sun, H.B. Quantum-confined-superfluidics-enabled moisture actuation based on unilaterally structured graphene oxide papers. *Adv. Mater.* **2019**, *31*, 1901585. [CrossRef] [PubMed]
2. Han, D.-D.; Zhang, Y.-L.; Ma, J.-N.; Liu, Y.-Q.; Han, B.; Sun, H.-B. Light-Mediated Manufacture and Manipulation of Actuators. *Adv. Mater.* **2016**, *28*, 8328–8343. [CrossRef]
3. Han, D.-D.; Zhang, Y.-L.; Jiang, H.-B.; Xia, H.; Feng, J.; Chen, Q.-D.; Xu, H.-L.; Sun, H.-B. Moisture-Responsive Graphene Paper Prepared by Self-Controlled Photoreduction. *Adv. Mater.* **2015**, *27*, 332–338. [CrossRef]
4. Mohammed, J.S.; Murphy, W.L. Bioinspired Design of Dynamic Materials. *Adv. Mater.* **2009**, *21*, 2361–2374. [CrossRef]
5. Liu, Y.Q.; Chen, Z.D.; Han, D.D.; Mao, J.W.; Ma, J.N.; Zhang, Y.L.; Sun, H.B. Bioinspired soft robots based on the moisture-responsive graphene oxide. *Adv. Sci.* **2021**, *8*, 2002464. [CrossRef] [PubMed]
6. Han, D.-D.; Cai, Q.; Chen, Z.-D.; Li, J.-C.; Mao, J.-W.; Lv, P.; Gao, B.-R. Bioinspired Surfaces with Switchable Wettability. *Front. Chem.* **2020**, *8*, 692. [CrossRef]
7. Zhang, Y.L.; Ma, J.N.; Liu, S.; Han, D.D.; Liu, Y.Q.; Chen, Z.D.; Mao, J.W.; Sun, H.B. A "Yin"-"Yang" complementarity strategy for design and fabrication of dual-responsive bimorph actuators. *Nano Energy* **2020**, *68*, 104302. [CrossRef]
8. Han, D.-D.; Liu, Y.-Q.; Ma, J.-N.; Mao, J.-W.; Chen, Z.-D.; Zhang, Y.-L.; Sun, H.-B. Biomimetic Graphene Actuators Enabled by Multiresponse Graphene Oxide Paper with Pretailored Reduction Gradient. *Adv. Mater. Technol.* **2018**, *3*, 1800258. [CrossRef]
9. Binetti, V.R.; Schiffman, J.D.; Leaffer, O.D.; Spanier, J.E.; Schauer, C.L. The natural transparency and piezoelectric response of the Greta oto butterfly wing. *Integr. Biol.* **2009**, *1*, 324–329. [CrossRef]
10. Wang, W.; Wang, G.P.; Zhang, W.; Zhang, D. Reversible thermochromic response based on photonic crystal structure in butterfly wing. *Nanophotonics* **2018**, *7*, 217–227. [CrossRef]
11. Wang, X.; Gu, C.; Wang, L.; Zhang, J.; Tu, J. Ionic liquids-infused slippery surfaces for condensation and hot water repellency. *Chem. Eng. J.* **2018**, *343*, 561–571. [CrossRef]
12. Wong, T.-S.; Kang, S.H.; Tang, S.K.Y.; Smythe, E.J.; Hatton, B.D.; Grinthal, A.; Aizenberg, J. Bioinspired self-repairing slippery surfaces with pressure-stable omniphobicity. *Nature* **2011**, *477*, 443–447. [CrossRef]
13. Xiao, L.; Li, J.; Mieszkin, S.; Di Fino, A.; Clare, A.S.; Callow, M.E.; Callow, J.A.; Grunze, M.; Rosenhahn, A.; Levkin, P. Slippery Liquid-Infused Porous Surfaces Showing Marine Antibiofouling Properties. *ACS Appl. Mater. Interfaces* **2013**, *5*, 10074–10080. [CrossRef]
14. Rykaczewski, K.; Anand, S.; Subramanyam, S.B.; Varanasi, K.K. Mechanism of Frost Formation on Lubricant-Impregnated Surfaces. *Langmuir* **2013**, *29*, 5230–5238. [CrossRef]
15. Su, B.; Guo, W.; Jiang, L. Learning from Nature: Binary Cooperative Complementary Nanomaterials. *Small* **2014**, *11*, 1072–1096. [CrossRef]
16. Yin, K.; Yang, S.; Dong, X.; Chu, D.; Duan, J.-A.; He, J. Robust laser-structured asymmetrical PTFE mesh for underwater directional transportation and continuous collection of gas bubbles. *Appl. Phys. Lett.* **2018**, *112*, 243701. [CrossRef]
17. Li, G.; Li, J.; Zhang, C.; Hu, Y.; Li, X.; Chu, J.; Huang, W.; Wu, D. Large-Area One-Step Assembly of Three-Dimensional Porous Metal Micro/Nanocages by Ethanol-Assisted Femtosecond Laser Irradiation for Enhanced Antireflection and Hydrophobicity. *ACS Appl. Mater. Interfaces* **2015**, *7*, 383–390. [CrossRef]
18. Yong, J.L.; Singh, S.C.; Zhan, Z.B.; ElKabbash, M.; Chen, F.; Guo, C.L. Femtosecond-laser-produced underwater "superpolymphobic" nanorippled surfaces: Repelling liquid polymers in water for applications of controlling polymer shape and adhe-sion. *ACS Appl. Nano Mater.* **2019**, *2*, 7362–7371. [CrossRef] [PubMed]
19. Fu, X.-Y.; Cai, Q.; Ma, J.-N.; Zhu, L.; Han, D.-D.; Zhang, Y.-L. Free-standing and flexible graphene supercapacitors of high areal capacitance fabricated by laser holography reduction of graphene oxide. *Appl. Phys. Lett.* **2021**, *118*, 071601. [CrossRef]
20. Liu, Y.-Q.; Mao, J.-W.; Chen, Z.-D.; Han, D.-D.; Jiao, Z.-Z.; Ma, J.-N.; Jiang, H.-B.; Yang, H. Three-dimensional micropatterning of graphene by femtosecond laser direct writing technology. *Opt. Lett.* **2020**, *45*, 113–116. [CrossRef]
21. Sugioka, K.; Cheng, Y. Femtosecond laser three-dimensional micro- and nanofabrication. *Appl. Phys. Rev.* **2014**, *1*, 041303. [CrossRef]
22. Vorobyev, A.Y.; Guo, C. Direct femtosecond laser surface nano/microstructuring and its applications. *Laser Photonics Rev.* **2013**, *7*, 385–407. [CrossRef]
23. Zhang, Y.-L.; Li, J.-C.; Zhou, H.; Liu, Y.-Q.; Han, D.-D.; Sun, H.-B. Electro-responsive actuators based on graphene. *Innovation* **2021**, *2*, 100168. [CrossRef] [PubMed]
24. Han, D.-D.; Chen, Z.-D.; Li, J.-C.; Mao, J.-W.; Jiao, Z.-Z.; Wang, W.; Zhang, W.; Zhang, Y.-L.; Sun, H.-B. Airflow Enhanced Solar Evaporation Based on Janus Graphene Membranes with Stable Interfacial Floatability. *ACS Appl. Mater. Interfaces* **2020**, *12*, 25435–25443. [CrossRef] [PubMed]

25. You, R.; Liu, Y.; Hao, Y.; Han, D.; Zhang, Y.; You, Z. Laser Fabrication of Graphene-Based Flexible Electronics. *Adv. Mater.* **2020**, *32*, e1901981. [CrossRef] [PubMed]
26. Han, D.-D.; Zhang, Y.-L.; Liu, Y.; Liu, Y.-Q.; Jiang, H.; Han, B.; Fu, X.-Y.; Ding, H.; Xu, H.-L.; Sun, H.-B. Bioinspired Graphene Actuators Prepared by Unilateral UV Irradiation of Graphene Oxide Papers. *Adv. Funct. Mater.* **2015**, *25*, 4548–4557. [CrossRef]
27. Wang, H.; Zhang, Y.L.; Han, D.D.; Wang, W.; Sun, H.B. Laser fabrication of modular superhydrophobic chips for recon-figurable assembly and self-propelled droplet manipulation. *PhotoniX* **2021**, *2*, 17. [CrossRef]
28. Zhao, R.; Huang, L.; Wang, Y. Recent advances in multi-dimensional metasurfaces holographic technologies. *PhotoniX* **2020**, *1*, 20. [CrossRef]
29. Qiao, Z.; Wan, Z.; Xie, G.; Wang, J.; Qian, L.; Fan, D. Multi-vortex laser enabling spatial and temporal encoding. *PhotoniX* **2020**, *1*, 1–14. [CrossRef]
30. Vorobyev, A.Y.; Topkov, A.N.; Gurin, O.V.; Svich, V.A.; Guo, C.L. Enhanced absorption of metals over ultrabroad electro-magnetic spectrum. *Appl. Phys. Lett.* **2009**, *95*, 121106. [CrossRef]
31. Fan, P.; Bai, B.; Jin, G.; Zhang, H.; Zhong, M. Patternable fabrication of hyper-hierarchical metal surface structures for ultrabroad-band antireflection and self-cleaning. *Appl. Surf. Sci.* **2018**, *457*, 991–999. [CrossRef]
32. Zheng, B.X.; Wang, W.J.; Jiang, G.D.; Mei, X.S. Fabrication of broadband antireflective black metal surfaces with ul-tra-light-trapping structures by picosecond laser texturing and chemical fluorination. *Appl. Phys. B Lasers Opt.* **2016**, *122*, 180. [CrossRef]
33. Murakami, D.; Jinnai, H.; Takahara, A. Wetting Transition from the Cassie–Baxter State to the Wenzel State on Textured Polymer Surfaces. *Langmuir* **2014**, *30*, 2061–2067. [CrossRef] [PubMed]